Power-Balanced Modelling Of Circuits As Skew Gradient Systems

Rémy Muller, Thomas Hélie

POWER-BALANCED MODELLING OF CIRCUITS AS SKEW GRADIENT SYSTEMS

Rémy Müller

IRCAM-STMS (UMR 9912)
Sorbonne University
Paris, France
remy.muller@ircam.fr

Thomas Hélie *

IRCAM-STMS (UMR 9912)
Sorbonne University
Paris, France
thomas.helie@ircam.fr

ABSTRACT

This article is concerned with the power-balanced simulation of analog audio circuits, governed by nonlinear differential algebraic equations (DAE). The proposed approach is to combine principles from the port-Hamiltonian and Brayton-Moser formalisms to yield a skew-symmetric gradient system. The practical interest is to provide a solver, using an average discrete gradient, that handles differential and algebraic relations in a unified way, and avoids having to pre-solve the algebraic part. This leads to a structure-preserving method that conserves the power balance and total energy. The proposed formulation is then applied on typical nonlinear audio circuits to study the effectiveness of the method.

1. INTRODUCTION

The need for stable, accurate and power-balanced simulation of nonlinear multi-physical systems is ubiquitous in the modelling of electronic circuits or mechanical systems and the natural setting for electronic circuits leads to Differential-Algebraic Equations.

Standard methods of solving electronic circuits are the State-variable [1], Modified Nodal Analysis [2], Sparse Tableau Analysis [3] and Wave Digital Filters (WDF) [4] according to the choice of variables the system is solved for. More recently, in the audio signal processing field, it has led to the Nodal DK method [5], nonlinear state-space [6] and extension of WDF to handle multi-port nonlinearities [7].

However, the underlying geometric structure and power-balance are often lost in the process. Furthermore, most numerical schemes either introduce or dissipate energy artificially, yielding unexpected, unstable or over-damped results.

To get rid of such artefacts, a very active research is focused on geometric numerical integration methods [8] that provide a theoretical framework for structure-preserving or invariant-preserving integration of dynamical systems. Among those methods, the Port-Hamiltonian (PHS) [9] [10] and Brayton-Moser (BM) [11] [12] formalisms are dual representations [13] [14] generalizing the Hamiltonian and Lagrangian formalisms to open dynamical systems with algebraic constraints (including dissipation).

PHS have been applied successfully to the modelling of the wah-wah pedal [15], Fender Rhodes [16], brass instruments [17] and loudspeaker nonlinearities [18]. Furthermore, automated generation of the PHS equations from the graph incidence matrix of a circuit's netlist has been investigated in [19] and leads to a skew-symmetric DAE form.

This paper considers this formulation as a starting point and proposes to combine the Brayton-Moser and Port-Hamiltonian viewpoints to represent all the constitutive laws as deriving from a single potential.

The presentation is organized as follows: first, in section 2, results about power balance, passivity, and duality of flow and effort spaces are recalled and it is shown how the power-balance can be represented by Dirac structures. Section 3 shows how, for both dynamic and algebraic components, the flow and effort variables can be derived from a single power potential involving the Hamiltonian and the algebraic content and co-content potentials [20] [21]. Section 4, then shows how to perform a power-balanced structure-preserving discretization of the system using a discrete gradient [22] [23]. Section 5 shows how to solve the resulting algebraic system using Newton iteration. Finally the method is applied to some example circuits in section 6 to show the effectiveness of the approach.

2. POWER BALANCE AND DIRAC STRUCTURES

For an electronic circuit, the Tellegen theorem [24] states that the sum of powers absorbed by all circuit elements is balanced.

$$P(\mathbf{e},\mathbf{f}) := \mathbf{e}^{\mathsf{T}}\mathbf{f} = \sum_n e_n f_n = 0 \tag{1}$$

where $\mathbf{e},\mathbf{f}$ are respectively the effort and flow variables of the circuit's branch components. This is an instance of the conservation of energy principle made famous by Lavoisier with the statement *nothing is lost, nothing is created, everything is transformed*.

This principle can be formalized mathematically by Dirac structures[1] that encodes the conservative power exchange in the circuit.

2.1. Power space

For an n-port element, let $\mathcal{F}$ be an n-dimensional real vector space and denote its dual $\mathcal{E} := \mathcal{F}^*$ (the space of linear functions on $\mathcal{F}$). We call $\mathcal{F}$ the space of flows $\mathbf{f}$ and $\mathcal{E}$ the space of efforts $\mathbf{e}$. On the product space $\mathcal{P} := \mathcal{F}\times\mathcal{E}$, power is defined by the non-degenerate bilinear form

$$P(\mathbf{e},\mathbf{f}) = \langle \mathbf{e} \,|\, \mathbf{f}\rangle, \quad \forall (\mathbf{f},\mathbf{e}) \in \mathcal{P} = \mathcal{F}\times\mathcal{E} \tag{2}$$

where $\langle \mathbf{e} \,|\, \mathbf{f}\rangle$ denotes the duality product, that is the linear function $\mathbf{e} \in \mathcal{E} = \mathcal{F}^*$ acting on $\mathbf{f} \in \mathcal{F}$. If $\mathcal{F}$ is equipped with an inner product $\langle\cdot,\cdot\rangle_{\mathcal{F}}$, then $\mathcal{E} = \mathcal{F}^*$ can be identified with $\mathcal{F}$ such that $\langle \mathbf{e} \,|\, \mathbf{f}\rangle = \langle \mathbf{e},\mathbf{f}\rangle_{\mathcal{F}}$, for all $\mathbf{f} \in \mathcal{F}$, $\mathbf{e} \in \mathcal{E} \sim \mathcal{F}$. If for example, $\mathcal{F}$ is the space of currents and $\mathcal{E}$ the space of voltages, then $\langle \mathbf{e} \,|\, \mathbf{f}\rangle = \langle \mathbf{e},\mathbf{f}\rangle_{\mathcal{F}} = \mathbf{e}^{\mathsf{T}}\mathbf{f}$ denote the electrical power.

* The author acknowledges the support of the ANR-DFG (French-German) project INFIDHEM ANR-16-CE92-0028.

[1] The Kirchoff Current and Voltage laws are special cases of Dirac structures when all the components share either the same current (series connection) or the same voltage (parallel connection).

2.2. Passivity and Dirac structures

In the $2n$-dimensional space $\mathcal{P}$, a passive linear n-port can be represented as an n-dimensional subspace $\mathcal{S} \subset \mathcal{P}$ defined by n linear constraints which admits the kernel representation

$$\mathcal{S} = \{(\mathbf{f}, \mathbf{e}) \in \mathcal{P} \mid \mathbf{F}\mathbf{f} + \mathbf{E}\mathbf{e} = 0\} \tag{3}$$

with $\mathrm{rank}([\mathbf{F}\ \mathbf{E}]) = n$. Furthermore, a linear subspace $\mathcal{D} \subset \mathcal{P}$ is said to be power-conserving if

$$\langle \mathbf{e} \,|\, \mathbf{f} \rangle = 0, \quad \forall (\mathbf{f}, \mathbf{e}) \in \mathcal{D} \tag{4}$$

It becomes a (constant) Dirac structure [25] [26] if and only if it is a maximal subspace of $\mathcal{P}$ with that property i.e. $\dim(\mathcal{D}) = \dim(\mathcal{F}) = \dim(\mathcal{E})$ and it admits the following matrix representations.

Definition 2.1 (Kernel representation)**.** *The kernel form of a Dirac structure is given by the subspace*

$$\mathcal{D} = \{(\mathbf{f}, \mathbf{e}) \in \mathcal{P} \mid \mathbf{F}\mathbf{f} + \mathbf{E}\mathbf{e} = 0,\ \mathbf{E}^\mathsf{T}\mathbf{F} + \mathbf{F}\mathbf{E}^\mathsf{T} = 0\} \tag{5}$$

where $\mathbf{F}, \mathbf{E} \in \mathbb{R}^{n\times n}$ *satisfy* $\mathrm{rank}([\mathbf{F}\ \mathbf{E}]) = n$.

Definition 2.2 (Hybrid skew-symmetric representation)**.** *Let* $\mathcal{D}$ *be given as in* (5)*, suppose there exists a permutation of the flow and efforts variables* $\pi : (\mathbf{F}, \mathbf{E}, \mathbf{f}, \mathbf{e}) \to (\tilde{\mathbf{F}}, \tilde{\mathbf{E}}, \tilde{\mathbf{f}}, \tilde{\mathbf{e}})$ *such that* $\tilde{\mathbf{F}}$ *is invertible then*

$$\mathcal{D} = \{(\tilde{\mathbf{f}}, \tilde{\mathbf{e}}) \in \mathcal{P} \quad | \quad \tilde{\mathbf{f}} = \mathbf{J}\tilde{\mathbf{e}}, \quad \mathbf{J} = -\tilde{\mathbf{F}}^{-1}\tilde{\mathbf{E}}\} \tag{6}$$

where $\mathbf{J} = -\mathbf{J}^\mathsf{T}$ *is skew-symmetric.*

Conversely, for any skew-symmetric matrix $\mathbf{J}$, the subspace $\mathcal{D}$ is a Dirac structure and one can verify that the power balance (1) is encoded by the skew-symmetry of $\mathbf{J}$:

$$P(\tilde{\mathbf{e}}, \tilde{\mathbf{f}}) = \tilde{\mathbf{e}}^\mathsf{T}\tilde{\mathbf{f}} = \tilde{\mathbf{e}}^\mathsf{T}\mathbf{J}\tilde{\mathbf{e}} = 0. \tag{7}$$

The skew-symetric form (6) will be used in the rest of the article.

3. GRADIENT DESCRIPTION OF COMPONENTS

Circuits are then categorized into dynamical, and algebraic components where algebraic components are further separated into dissipative and external sources because the later have degenerated constitutive laws. We show how the mixed effort $\tilde{\mathbf{e}}$ can be uniformly represented as the gradient of the scalar power potential (1).

3.1. Dynamic components: Hamiltonian potential

For dynamic components with state variable $\mathbf{x}$, flow variables are defined as the time-derivative of the state ($\mathbf{f} := \dot{\mathbf{x}}$) and the effort by a constitutive law $\mathbf{e} := \hat{e}(\mathbf{x})$. It is assumed that the constitutive law derives from the gradient of an energy storage function $H(\mathbf{x}(t))$ such that by definition $\hat{e}(\mathbf{x}) := \nabla H(\mathbf{x})$ and the power is

$$P(\mathbf{e}, \mathbf{f}) = \mathbf{e}^\mathsf{T}\mathbf{f} = \nabla H(\mathbf{x}) \cdot \dot{\mathbf{x}} = \frac{\mathrm{d}}{\mathrm{d}t} H(\mathbf{x}(t)). \tag{8}$$

The Hamiltonian function can then be found using the line integral.

$$H(\mathbf{x}) = \int \underbrace{\nabla H(\mathbf{x})}_{\mathbf{e}} \cdot \underbrace{\dot{\mathbf{x}}}_{\mathbf{f}} \,\mathrm{d}t = \int \nabla H(\mathbf{x}) \cdot \mathrm{d}\mathbf{x} \tag{9}$$

This idea is illustrated with the important cases of the linear capacitor and inductor. We then show how to handle a nonlinear component with an integrable constitutive law.

3.1.1. Capacitor

For a capacitor, the state variable is given by the charge $x_C = q$, with the flow $f = i_C = \dot{q}$, and effort $e = v_C = \frac{q}{C}$. This gives the Hamiltonian

$$H(q) = \int \frac{q}{C} \cdot \dot{q}\,\mathrm{d}t = \frac{1}{C}\int q\,\mathrm{d}q = \frac{q^2}{2C} \tag{10}$$

3.1.2. Inductor

Similarily for an inductor, the state variable is given by the flux-linkage $x_L = \phi$, the flow[2] by its time-derivative $f = \dot{\phi} = v_L$ and the dual effort by $e = i_L = \frac{\phi}{L}$ with an Hamiltonian function

$$H(\phi) = \int \frac{\phi}{L} \cdot \dot{\phi}\,\mathrm{d}t = \frac{1}{L}\int \phi \cdot \mathrm{d}\phi = \frac{\phi^2}{2L} \tag{11}$$

3.1.3. Nonlinear dynamic component

For a nonlinear dynamic component with state variable x, flow $f = \dot{x}$ and a constitutive law $e = \hat{e}(x) = \tanh(x)$, its Hamiltonian storage function is given by

$$H(x) = \int_0^t \hat{e}(x) \cdot \dot{x}\,\mathrm{d}t = \int_0^x \hat{e}(\bar{x}) \cdot \mathrm{d}\bar{x} = \ln(\cosh(x)) \tag{12}$$

3.2. Algebraic components: current and voltage potentials

If we consider the power differential $\mathrm{d}P$, using the product rule,

$$\mathrm{d}P(\mathbf{e}, \mathbf{f}) = \mathrm{d}(\mathbf{e} \cdot \mathbf{f}) = \mathbf{e} \cdot \mathrm{d}\mathbf{f} + \mathbf{f} \cdot \mathrm{d}\mathbf{e}. \tag{13}$$

Integration over a path Γ gives the integration by parts formula

$$\mathbf{e} \cdot \mathbf{f}\Big|_{\partial\Gamma} = \int_\Gamma \mathbf{e} \cdot \mathrm{d}\mathbf{f} + \int_\Gamma \mathbf{f} \cdot \mathrm{d}\mathbf{e}. \tag{14}$$

So, for components defined by algebraic constitutive laws $\Gamma = \{(\mathbf{e}, \mathbf{f}) \in \mathcal{P} \mid \mathbf{f} = \hat{f}(\mathbf{e})\}$, (respectively $\mathbf{e} = \hat{e}(\mathbf{f})$), the flow and effort potentials[3] are defined by the line integrals

$$D(\mathbf{f}) := \int_0^{\mathbf{f}} \hat{e}(\bar{\mathbf{f}}) \cdot \mathrm{d}\bar{\mathbf{f}}, \qquad D^*(\mathbf{e}) := \int_0^{\mathbf{e}} \hat{f}(\bar{\mathbf{e}}) \cdot \mathrm{d}\bar{\mathbf{e}}. \tag{15}$$

And according to (14), the instantaneous power is given, for $(\mathbf{e}, \mathbf{f}) \in \Gamma$, by (see figure 1 for a geometric interpretation and proof)

$$P(\mathbf{e}, \mathbf{f}) = \mathbf{e} \cdot \mathbf{f} = D(\mathbf{f}) + D^*(\mathbf{e}). \tag{16}$$

The flow and efforts can then be respectively obtained by partial derivatives of the power potential as

$$\mathbf{e} = \frac{\partial P}{\partial \mathbf{f}} = \nabla D(\mathbf{f}), \qquad \text{or} \qquad \mathbf{f} = \frac{\partial P}{\partial \mathbf{e}} = \nabla D^*(\mathbf{e}). \tag{17}$$

So in the case of a flow (resp. effort) controlled component the power can be expressed as a function of a single variable using either

$$P(\mathbf{e}) = \mathbf{e} \cdot \nabla D^*(\mathbf{e}) \qquad \text{or} \qquad P(\mathbf{f}) = \nabla D(\mathbf{f}) \cdot \mathbf{f}. \tag{18}$$

[2] Note that according to the energy domain (electric, magnetic, ...), the roles of flow and efforts need not necessarily be associated to the current and voltage. The convention adopted here, is that the flow of dynamic components is given by the time-derivative of the energy variable, while the effort is given by the gradient of the energy potential.

[3] These potentials are also called the content and co-content [20] [21].

3.2.1. Linear resistor

For a current-controlled (resp. voltage-controlled) resistor, the constitutive law is $v = \hat{e}(i) = Ri$ (resp. $i = \hat{f}(v) = v/R$). By consequence its current and voltage potentials are given by

$$D(i) = \int_0^i \hat{e}(f)\,\mathrm{d}f = \int_0^i Rf\,\mathrm{d}f = \frac{Ri^2}{2} \tag{19}$$

$$D^*(v) = \int_0^v \hat{f}(e)\,\mathrm{d}e = \int_0^v \frac{e}{R}\,\mathrm{d}e = \frac{v^2}{2R}. \tag{20}$$

Introduce function P as $P(v,i) = D(i) + D^*(v)$, then, for all (v,i) belonging on the characteristic curve, the power can be given by $v \cdot i$ (product-type), $P(v,i)$ (sum-type), $P(v,\hat{f}(v))$ (voltage-controlled) and $P(\hat{e}(i),i)$ (current-controlled), that is

$$P(v,i) = v{\cdot}i = D(i){+}D^*(v) = \frac{1}{2}\left(Ri^2 + \frac{v^2}{R}\right) = \frac{v^2}{R} = Ri^2. \tag{21}$$

In this particular case, we have $D(i) = D^*(v) = Ri^2$ because of linearity (for $v = Ri$) but this result should not be extrapolated as the next example will show.

3.2.2. P-N Diode

For a voltage controlled P-N diode, the constitutive law is given by

$$i = \hat{f}(v) = I_S\left(\exp\left(\frac{v}{nV_T}\right) - 1\right) \tag{22}$$

where I_S is the saturation current, n the ideality factor and V_T the thermal voltage. Its voltage potential is given by

$$D^*(v) = \int_0^v \hat{f}(e)\,\mathrm{d}e = nV_T I_S\left(\exp\left(\frac{v}{nV_T}\right) - \frac{v}{nV_T} - 1\right). \tag{23}$$

Direct integration for the current potential does not lead to an easily integrable primitive, however because of bijectivity, we can evaluate it indirectly by using the inverse map

$$v = \hat{e}(i) = \hat{f}^{-1}(i) = nV_T \ln\left(1 + \frac{i}{I_S}\right), \quad i > -I_S \tag{24}$$

and the Legendre transform $D(i) = \left[vi - D^*(v)\right]_{v=\hat{f}^{-1}(i)}$:

$$D(i) = nV_T I_S\left(\left(1 + \frac{i}{I_S}\right)\ln\left(1 + \frac{i}{I_S}\right) - \frac{i}{I_S}\right) \tag{25}$$

Using the above definitions, the current and voltage potentials being known, the component can be used as being either flow or effort-driven according to the constraints imposed by the circuit interconnections.

3.3. External sources

For external voltage (resp. current) sources, the constitutive laws $v = \hat{e}(i) = V$, (resp. $i = \hat{f}(v) = I$) are independent of the current (resp. voltage) variables and not bijective, with V (resp. I) being the source parameter. This gives the powers

$$P_V(v,i) = Vi = D(i), \qquad P_I(v,i) = vI = D^*(v). \tag{26}$$

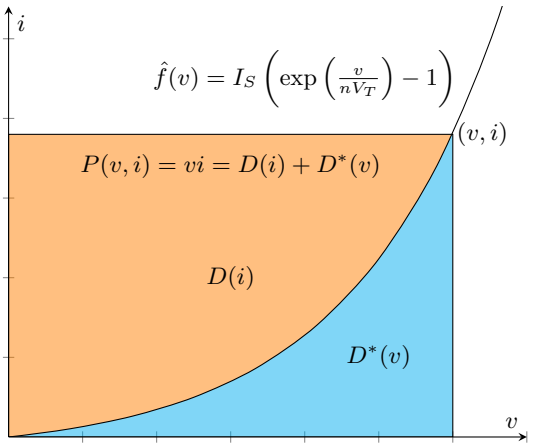

Figure 1: The areas occupied by the diode power $P(v,i)$ and the current and voltage potentials $D(i)$ and $D^*(v)$ are shown in the (v,i) plane for $I_S = 1, nV_T = 1$. It is geometrically clear that the current and voltage potentials are complimentary and their sum equals the power vi. It is also clear that in the nonlinear case $D(i) \neq D^*(v)$.

By consequence, for voltage (resp. current) sources, the voltage potential $D^*(v)$ (resp. current potential $D(i)$) is degenerate and null.

3.4. Summary

Using an appropriate permutation π (cf definition 2.2), the mixed flow $\tilde{\mathbf{f}}$ and its dual $\tilde{\mathbf{e}}$ can be parametrized by a state variable $\mathbf{x} \in \mathbb{R}^n$, a dissipative variable $\mathbf{w} \in \mathbb{R}^p$ and an output $\mathbf{y} \in \mathbb{R}^m$, where the potential $Z(\mathbf{w})$ (resp. $S(\mathbf{y})$) is an appropriate choice among the dissipative (resp. external) current and voltage potentials imposed by the permutation π. (Please refer to [19] for more details.)

$$\tilde{\mathbf{f}} := [\dot{\mathbf{x}}, \mathbf{w}, \mathbf{y}]^\mathsf{T} \tag{27}$$

$$\tilde{\mathbf{e}} := [\nabla H(\mathbf{x}), \nabla Z(\mathbf{w}), \nabla S(\mathbf{y})]^\mathsf{T} \tag{28}$$

The power potential[4] (1) can then be expressed as

$$P(\tilde{\mathbf{e}}, \tilde{\mathbf{f}}) = \tilde{\mathbf{e}}^\mathsf{T}\tilde{\mathbf{f}} = \underbrace{\nabla H(\mathbf{x})^\mathsf{T}\dot{\mathbf{x}}}_{P_c} + \underbrace{\nabla Z(\mathbf{w})^\mathsf{T}\mathbf{w}}_{P_d} + \underbrace{\nabla S(\mathbf{y})^\mathsf{T}\mathbf{y}}_{P_e}. \tag{29}$$

Combining the definitions (27) and (28), with the Dirac structure (6), leads to the skew-symmetric gradient form of Differential-Algebraic Port-Hamiltonian equations as

$$\underbrace{\begin{bmatrix}\dot{\mathbf{x}}\\ \mathbf{w}\\ \mathbf{y}\end{bmatrix}}_{\tilde{\mathbf{f}}} = \mathbf{J}\underbrace{\begin{bmatrix}\nabla H(\mathbf{x})\\ \nabla Z(\mathbf{w})\\ \nabla S(\mathbf{y})\end{bmatrix}}_{\tilde{\mathbf{e}}} \quad \Longleftrightarrow \quad \frac{\partial P}{\partial \tilde{\mathbf{e}}} = \mathbf{J}\frac{\partial P}{\partial \tilde{\mathbf{f}}} \tag{30}$$

[4] Note that because of the uniform usage of the *receiver convention* for each component (including sources), the power potentials represent the *absorbed* power by each component. This means that dissipative components will absorb *positive power*, while sources will, on average, absorb *negative power* to compensate for losses (but can temporarily receive power).

Integrating (29) over a time interval $[t_0, t_1]$ combined with the power balance (7), leads to the conservation of the total energy

$$\Delta E = H(\mathbf{x})\Big|_{t_0}^{t_1} + \int_{t_0}^{t_1} P_d(t)\,\mathrm{d}t + \int_{t_0}^{t_1} P_e(t)\,\mathrm{d}t = 0. \quad (31)$$

4. STRUCTURE-PRESERVING INTEGRATION SCHEME

The main objective of the numerical scheme is first and foremost, to provide a structure-preserving method that conserves the invariant (31) in discrete-time over each time-step. This offers the strong guarantee that no artificial energy is either consumed or created by the numerical scheme.To achieve this goal, thanks to the unified representation of DAE circuits as gradient systems introduced in section 3, it is now possible to generalize the usage of discrete gradient methods [22] [23] for *both* dynamic and algebraic components.

4.1. Discrete Gradients

Given a scalar potential $H : \mathbb{R}^n \mapsto \mathbb{R}$, a point $\mathbf{x} \in \mathbb{R}^n$ and a variation $\delta\mathbf{x} \in \mathbb{R}^n$, a necessary and sufficient condition for a function $\overline{\nabla} H(\mathbf{x}, \delta\mathbf{x}) : \mathbb{R}^n \times \mathbb{R}^n \mapsto \mathbb{R}^n$ to be a discrete gradient is given by

$$\overline{\nabla} H(\mathbf{x}, \delta\mathbf{x}) \cdot \delta\mathbf{x} = H(\mathbf{x} + \delta\mathbf{x}) - H(\mathbf{x}) \quad (32)$$

$$\overline{\nabla} H(\mathbf{x}, 0) = \nabla H(\mathbf{x}) \quad (33)$$

Definition 4.1 (Average Discrete Gradient)**.** *Let $\mathbf{x}, \delta\mathbf{x} \in \mathbb{R}^n$, and $H : \mathbb{R}^n \mapsto \mathbb{R}$ be a scalar potential. The average discrete gradient is defined for an affine trajectory model $\hat{\mathbf{x}}(\tau) = \mathbf{x} + \tau\delta\mathbf{x}$ by*

$$\overline{\nabla} H(\mathbf{x}, \delta\mathbf{x}) := \int_0^1 \nabla H(\mathbf{x} + \tau\delta\mathbf{x})\,\mathrm{d}\tau \quad (34)$$

Furthermore, using the gradient theorem, for separable potentials of the form

$$H(\mathbf{x}) = \sum_{i=1}^{N} H_i(x_i), \quad (35)$$

the discrete gradient can be computed *exactly* by finite differences on each scalar potential. It is given component-wise by

$$[\overline{\nabla} H(\mathbf{x}, \delta\mathbf{x})]_i := \begin{cases} \dfrac{H_i(x_i + \delta x_i) - H_i(x_i)}{\delta x_i} & \delta x_i \neq 0 \\ \dfrac{\partial H_i}{\partial x_i}(x_i) & \delta x_i = 0 \end{cases} \quad (36)$$

Finally, and *only in the case of quadratic potentials* of the form $H(\mathbf{x}) = \frac{1}{2}\mathbf{x}^T\mathbf{W}\mathbf{x}$ with $\mathbf{W} = \mathbf{W}^T \succeq 0$, does the discrete gradient correspond to evaluation of the gradient at the mid-point.

$$\overline{\nabla} H(\mathbf{x}, \delta\mathbf{x}) = \nabla H\left(\mathbf{x} + \frac{1}{2}\delta\mathbf{x}\right) = \mathbf{W}\left(\mathbf{x} + \frac{1}{2}\delta\mathbf{x}\right) \quad (37)$$

The following result will also be exploited in the next section.

Property 4.1. *Given a separable potential $H : \mathbb{R}^n \mapsto \mathbb{R}$, as in* (35) *of class $\mathcal{C}^2$, a point $\mathbf{x} \in \mathbb{R}^n$, a variation $\boldsymbol{\nu} \in \mathbb{R}^n$ and its discrete gradient $\overline{\nabla} H(\mathbf{x}, \boldsymbol{\nu})$ defined as* (36)*, the derivative of the discrete gradient with respect to the variation $\boldsymbol{\nu}$ is the diagonal matrix $\partial_{\boldsymbol{\nu}} \overline{\nabla} H : (\mathbf{x}, \boldsymbol{\nu}) \in \mathbb{R}^n \times \mathbb{R}^n \to \mathbb{R}^{n\times n}$ with entries*

$$\left[\partial_{\boldsymbol{\nu}} \overline{\nabla} H\right]_{i,i} = \begin{cases} \dfrac{\nabla H_i(x_i + \nu_i) - \overline{\nabla} H_i(x_i, \nu_i)}{\nu_i} & \nu_i \neq 0 \\ \dfrac{1}{2}\dfrac{\partial^2 H_i}{\partial x_i^2}(x_i) & \nu_i = 0 \end{cases} \quad (38)$$

Proof. see Appendix A. □

4.2. Averaged System

Assuming over each time step $\Omega_n = [t_n, t_n + h]$, an affine trajectory model

$$\mathbf{z}(t_n + h\tau) = \mathbf{z}_n + \tau\delta\mathbf{z}_n \quad (39)$$

where $\mathbf{z} = [\mathbf{x}, \mathbf{w}, \mathbf{y}]^T$, and integrating (30) over Ω_n, we obtain the discrete structure-preserving system

$$\begin{bmatrix} \delta\mathbf{x}_n/h \\ \bar{\mathbf{w}}_n \\ \bar{\mathbf{y}}_n \end{bmatrix} = \mathbf{J} \begin{bmatrix} \overline{\nabla} H(\mathbf{x}_n, \delta\mathbf{x}_n) \\ \overline{\nabla} Z(\mathbf{w}_n, \delta\mathbf{w}_n) \\ \overline{\nabla} S(\mathbf{y}_n, \delta\mathbf{y}_n) \end{bmatrix} \quad (40)$$

where $\bar{\mathbf{w}}_n = \mathbf{w}_n + \delta\mathbf{w}_n/2$, $\bar{\mathbf{y}}_n = \mathbf{y}_n + \delta\mathbf{y}_n/2$. The DAE system (30) has been converted to an algebraic system that needs to be to solved for the average variation $\delta\mathbf{z}_n = [\delta\mathbf{x}_n, \delta\mathbf{w}_n, \delta\mathbf{y}_n]^\mathsf{T}$.

5. NEWTON ITERATION

Denote the variation $\boldsymbol{\nu} = \delta\mathbf{z}_n$, solving the discrete algebraic system (40) can be rewritten as the root-finding problem

$$F(\boldsymbol{\nu}^*) = 0 \quad (41)$$

where $\boldsymbol{\nu}^*$ is the looked for solution and F is defined by

$$F(\boldsymbol{\nu}) := \mathbf{D}_0\mathbf{z}_n + \mathbf{D}_1\boldsymbol{\nu} - \mathbf{J}\overline{\nabla}_{\tilde{\mathbf{f}}} P(\mathbf{z}_n, \boldsymbol{\nu}), \quad (42)$$

with $\mathbf{D}_0 = \begin{bmatrix} 0 & 0 & 0 \\ 0 & \mathbf{I}_p & 0 \\ 0 & 0 & \mathbf{I}_m \end{bmatrix}$, $\mathbf{D}_1 = \begin{bmatrix} \mathbf{I}_n/h & 0 & 0 \\ 0 & \mathbf{I}_p/2 & 0 \\ 0 & 0 & \mathbf{I}_m/2 \end{bmatrix}$, where $\mathbf{I}_n$ denote the $n \times n$ identity matrix and $\overline{\nabla}_{\tilde{\mathbf{f}}} P = [\overline{\nabla} H, \overline{\nabla} Z, \overline{\nabla} S]^\mathsf{T}$.

5.1. Newton update

For an estimate $\boldsymbol{\nu}_k$ and a perturbation $\Delta\boldsymbol{\nu}_k$, the true solution $\boldsymbol{\nu}^*$ of (41) can be written as $\boldsymbol{\nu}^* = \boldsymbol{\nu}_k + \Delta\boldsymbol{\nu}_k$. Taylor series expansion of F around $\boldsymbol{\nu}_k$, with $\|\Delta\boldsymbol{\nu}_k\|$ sufficiently small yields

$$0 = F(\boldsymbol{\nu}_k + \Delta\boldsymbol{\nu}_k) = F(\boldsymbol{\nu}_k) + [F'(\boldsymbol{\nu}_k)](\Delta\boldsymbol{\nu}_k) + \mathcal{O}(\|\Delta\boldsymbol{\nu}_k\|^2). \quad (43)$$

If the Jacobian F' is invertible, neglecting high-order terms and solving for $\Delta\boldsymbol{\nu}$ leads to the Newton update

$$\Delta\boldsymbol{\nu}_k := -F'(\boldsymbol{\nu}_k)^{-1} F(\boldsymbol{\nu}_k), \quad \boldsymbol{\nu}_{k+1} := \boldsymbol{\nu}_k + \Delta\boldsymbol{\nu}_k, \quad (44)$$

where the Jacobian of F is given by

$$F'(\boldsymbol{\nu}) = \mathbf{D}_1 - \mathbf{J}\left(\partial_{\boldsymbol{\nu}} \overline{\nabla}_{\tilde{\mathbf{f}}} P(\mathbf{z}_n, \boldsymbol{\nu})\right). \quad (45)$$

For a separable potential P, using property (4.1), $\partial_{\boldsymbol{\nu}} \overline{\nabla}_{\tilde{\mathbf{f}}} P$ is a diagonal matrix that can be computed from the knowledge of the gradient, Hessian and discrete gradient of the potential.

5.2. Convergence and stiffness

If the eigenvalues of the matrix $\mathbf{A} = \mathbf{D}_1^{-1}\mathbf{J}\left(\partial_{\boldsymbol{\nu}}\overline{\nabla}_{\tilde{\mathbf{f}}}P(\mathbf{z}_n,\boldsymbol{\nu})\right)$ are such that $\|\mathbf{A}\|_2 = \max(|\lambda_i|) < 1$, the fixed-point induced by (40) is contracting. The Banach fixed-point theorem guarantees existence and unicity of the solution. It is then possible to approximate the inverse of the Jacobian with the Neumann series identity

$$(\mathbf{I}-\mathbf{A})^{-1} = \sum_{k=0}^{\infty}\mathbf{A}^k \approx \mathbf{I}+\mathbf{A}+\mathbf{A}^2+\dots \tag{46}$$

to get the first (or any higher) order approximation

$$F'(\boldsymbol{\nu})^{-1} \approx \left(\mathbf{I}+\mathbf{D}_1^{-1}\mathbf{J}\left(\partial_{\boldsymbol{\nu}}\overline{\nabla}_{\tilde{\mathbf{f}}}P(\mathbf{z}_n,\boldsymbol{\nu})\right)\right)\mathbf{D}_1^{-1} \tag{47}$$

If $\max|\lambda_i| \geq 1$, the system is said to be stiff, the series (46) is divergent, and the approximation (47) is no longer valid. Solving the system then requires a matrix inversion for each iteration. Using the Newton-Kantorovich theorem, for a starting point $\boldsymbol{\nu}_0$, if there exists positive constants β_0, γ, h_0, such that $\|F'(\boldsymbol{\nu}_0)^{-1}\| \leq \beta_0$, $F'(\boldsymbol{\nu})$ is locally γ-Lipschitz and $h_0 := \|\Delta\boldsymbol{\nu}_0\|\,\beta_0\gamma < 1/2$, then the sequence $\{\boldsymbol{\nu}_k\}$ converges quadratically to some unique $\boldsymbol{\nu}^*$ such that $F(\boldsymbol{\nu}^*) = 0$. Please refer to [27] for more details.

6. CIRCUIT EXAMPLES

6.1. Envelope Follower

We consider the envelope follower circuit shown in figure 3 with parameters $C = 100$ pF, $I_S = 2.52$ nA, $V_T = 23$ mV and $n = 1.96$. Kirchoff laws leads to the following Dirac structure:

$$\underbrace{\begin{bmatrix} i_C \\ v_D \\ i_S \end{bmatrix}}_{\tilde{\mathbf{f}}} = \underbrace{\begin{bmatrix} 0 & 1 & 0 \\ -1 & 0 & 1 \\ 0 & -1 & 0 \end{bmatrix}}_{\mathbf{J}} \underbrace{\begin{bmatrix} v_C \\ i_D \\ v_S \end{bmatrix}}_{\tilde{\mathbf{e}}}. \tag{48}$$

For this circuit we have $\mathbf{x} = [q]$, $\mathbf{w} = [v_D]$, $\mathbf{y} = [i_S]$, $\tilde{\mathbf{f}} = [\dot{q}, v_D, i_S]^\mathsf{T}$ and the following potentials

$$H(q) = \frac{q^2}{2C}, \tag{49}$$

$$Z(v_D) = nV_TI_S\left(\exp\left(\frac{v_D}{nV_T}\right)-1\right) - v_DI_S, \tag{50}$$

$$S(i_S) = Vi_S. \tag{51}$$

Taking their gradients gives the right-hand side vector

$$\tilde{\mathbf{e}} = \begin{bmatrix} v_C \\ i_D \\ v_S \end{bmatrix} = \begin{bmatrix} \nabla H(q) \\ \nabla Z(v_D) \\ \nabla S(i_S) \end{bmatrix} = \begin{bmatrix} q/C \\ I_S\left(\exp\left(\frac{v_D}{nV_T}\right)-1\right) \\ V \end{bmatrix} \tag{52}$$

and the product $\tilde{\mathbf{e}}^\mathsf{T}\tilde{\mathbf{f}}$ gives the power balance potential

$$P(\tilde{\mathbf{e}},\tilde{\mathbf{f}}) = \underbrace{\nabla H(q)\dot{q}}_{P_C(q)} + \underbrace{\nabla Z(v_D)v_D}_{P_D(v_D)} + \underbrace{\nabla S(i_S)i_S}_{P_S(i_S)}. \tag{53}$$

For the capacitor and voltage source, we obtain the discrete gradients

$$\overline{\nabla}H(q,\delta q) = \frac{1}{C}\left(q+\frac{\delta q}{2}\right), \qquad \overline{\nabla}S(i,\delta i) = V, \tag{54}$$

and after some algebraic manipulations (see appendix B), the discrete gradient of the diode potential can be expressed as

$$\overline{\nabla}Z(v,\delta v) = I_S\left(\exp\left(\frac{v+\delta v/2}{nV_T}\right)\operatorname{sinhc}\left(\frac{\delta v}{2nV_T}\right)-1\right). \tag{55}$$

where the sinhc term ($\operatorname{sinhc} := \sinh(x)/x$) acts as a correction compared to evaluation of the gradient at the mid-point.

6.2. Diode Clipper

We consider the diode clipper circuit shown in figure 5 with parameters $R = 1$ kΩ, $C = 100$ nF, $I_S = 2.52$ fA, $V_T = 23$ mV and $n = 1$. For the two diodes, with $v_D := v_{D_1}$ and the diodes current $i_D := i_{D_1} - i_{D_2}$, the constitutive law is

$$i_D = \hat{f}(v_D) = 2I_S\sinh\left(\frac{v_D}{nV_T}\right). \tag{56}$$

Its integration gives the voltage potential

$$D_D^*(v_D) = \int_0^{v_D}\hat{f}(v)dv = 2nV_TI_S\left(\cosh\left(\frac{v_D}{nV_T}\right)-1\right). \tag{57}$$

Application of Kirchoff laws leads to the following Dirac structure:

$$\underbrace{\begin{bmatrix} i_C \\ v_R \\ v_D \\ i_S \end{bmatrix}}_{\tilde{\mathbf{f}}} = \underbrace{\begin{bmatrix} 0 & 1 & -1 & 0 \\ -1 & 0 & 0 & 1 \\ 1 & 0 & 0 & 0 \\ 0 & -1 & 0 & 0 \end{bmatrix}}_{\mathbf{J}} \underbrace{\begin{bmatrix} v_C \\ i_R \\ i_D \\ v_S \end{bmatrix}}_{\tilde{\mathbf{e}}}. \tag{58}$$

For this circuit, $\mathbf{x} = [q]$, $\mathbf{w} = [v_R, v_D]^\mathsf{T}$, $\mathbf{y} = [i_S]$, $\tilde{\mathbf{f}} = [\dot{q}, v_R, v_D, i_S]^\mathsf{T}$ and the potentials are

$$H(q) = \frac{q^2}{2C}, \quad Z(v_R,v_D) = \frac{v_R^2}{2R} + D_D^*(v_D), \quad S(i_S) = Vi_S. \tag{59}$$

Their gradients regenerates the mixed effort

$$\tilde{\mathbf{e}} = \begin{bmatrix} v_C \\ i_R \\ i_D \\ v_S \end{bmatrix} = \begin{bmatrix} \nabla H \\ \nabla Z_R \\ \nabla Z_D \\ \nabla S \end{bmatrix} = \begin{bmatrix} q/C \\ v_R/R \\ 2I_S\sinh\left(\frac{v_D}{nV_T}\right) \\ V \end{bmatrix} \tag{60}$$

and the product $\tilde{\mathbf{e}}^\mathsf{T}\tilde{\mathbf{f}}$ gives the power balance potential

$$P(\tilde{\mathbf{e}},\tilde{\mathbf{f}}) = \underbrace{\nabla H(q)\dot{q}}_{P_C(q)} + \underbrace{\nabla Z_R(v_R)v_R}_{P_R(v_R)} + \underbrace{\nabla Z_D(v_D)v_D}_{P_D(v_D)} + \underbrace{\nabla S(i_S)i_S}_{P_S(i_S)}. \tag{61}$$

Similarily as in the envelope follower case, we have the discrete gradients (54) for the capacitor and voltage source, with

$$\overline{\nabla}Z_R(v,\delta v) = \frac{1}{R}\left(v+\frac{\delta v}{2}\right) \tag{62}$$

for the resistor, and after some algebraic manipulations, the discrete gradient of the diodes potential can be expressed as

$$\overline{\nabla}Z_D(v,\delta v) = 2I_S\sinh\left(\frac{v+\delta v/2}{nV_T}\right)\operatorname{sinhc}\left(\frac{\delta v}{2nV_T}\right). \tag{63}$$

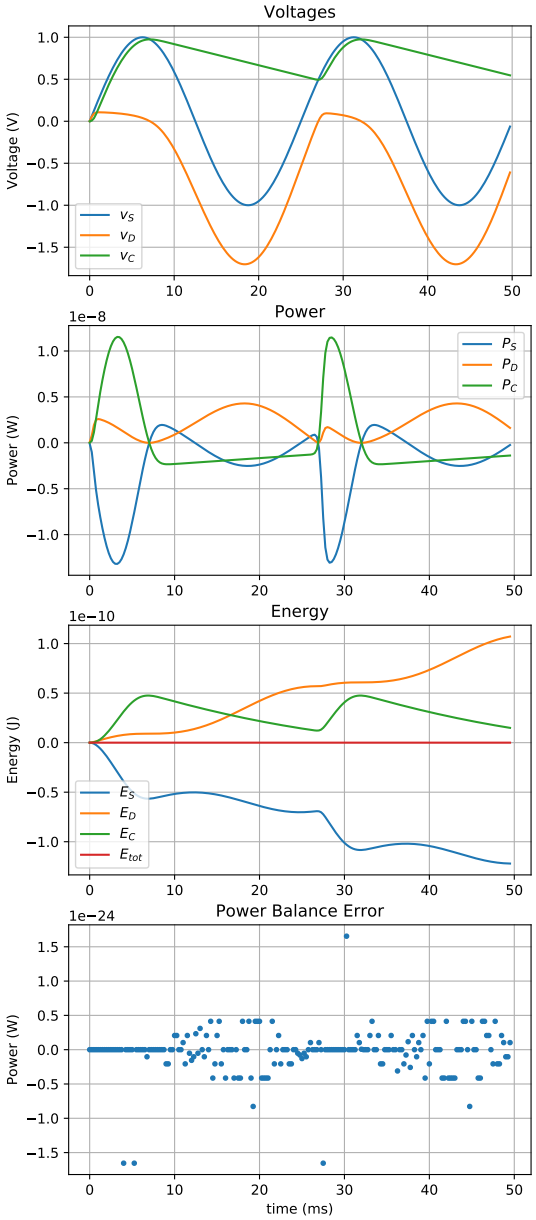

Figure 2: Envelope follower circuit driven by a 1V sinusoidal input with fundamental frequency $f = 40$ Hz, $f_s = 4$ kHz.

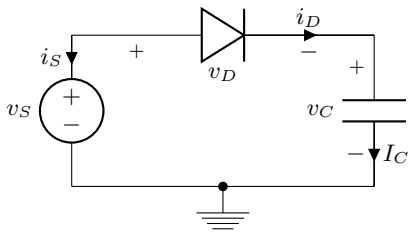

Figure 3: Envelope Follower circuit

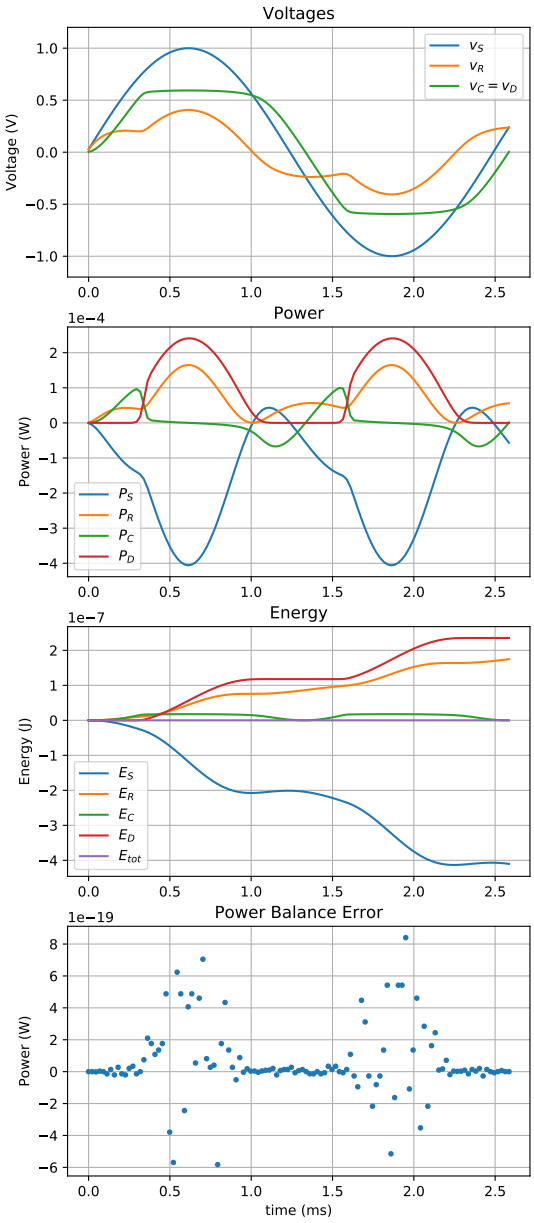

Figure 4: Diode clipper circuit driven by a 1V sinusoidal input with fundamental frequency $f = 400$ Hz, $f_s = 44.1$ kHz.

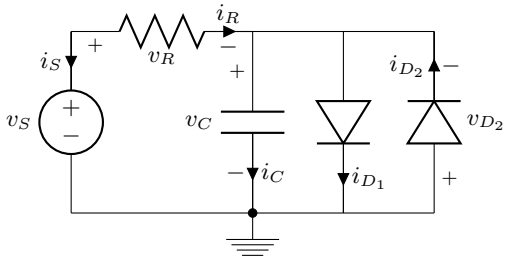

Figure 5: Diode Clipper circuit

6.3. Analysis

Simulation results for both circuits are shown in figure 2 and figure 4 with respective sampling frequencies 4 kHz and 44.1 kHz. We remark that in both cases, the power balance is satisfied with high precision. The relative error is of the order of the machine epsilon ($\epsilon = 2^{-53} \approx 1.11 \cdot 10^{-16}$). This results in a vanishing total energy variation.

For dissipative components, the absorbed power is always positive; the dissipated energy is thus monotonously increasing. For dynamic components and sources, the power is alternatively absorbed and released, the difference being that sources have a decreasing average energy trend to compensate for losses in the dissipative components.

Existence and uniqueness of the fixed points are guaranteed if $h < C/\gamma_D$ for the envelope follower and if $h < C/\max(\gamma_D, \gamma_R)$ for the diode clipper (proof is ommited) where γ_K stands for the local Lipschitz constants $\gamma_K = \max_\nu |\partial_\nu \overline{\nabla} Z_K(v_{K_0}, \nu)|$ of the diode and resistor components in a neighborhood around $\boldsymbol{\nu}_0$.

For the diode clipper circuit, the fixed-point does not converge, but the Newton iteration does. We can remark that each time the diodes are saturating, the precision of the power balance is slightly deteriorated. This can be explained by two facts: the dissipated power is also increasing during saturation and the system becomes stiff, thus the numerical conditioning of the Jacobian in the Newton iteration gets worse.

7. CONCLUSION

The main contribution of this paper consists in a) using the power-balance as the core object from which all quantities in the system are derived, b) generalizing the usage of potentials and their gradients to represent the flow and effort variables for both dynamic an algebraic components, c) keeping the sparse skew-symmetric structure matrix $\mathbf{J}$ until numerical simulation, d) integration of the system using the average discrete gradient. This leads to a consistent structure-preserving approximation that conserves the form of the original system in discrete-time.

It is also shown that the Jacobian of the Newton iteration has a special structure that only involves diagonal and skew-symmetric matrices. It can be computed only from the knowledge of the potentials associated with each component and stiffness can be inferred by inspection of the derivatives of the discrete gradient. Furthermore the structure-preserving approach offers a valuable tool to monitor the quality of our approximations with respect to the power balance.

The main drawback of the approach is a direct consequence from its strength. Indeed, the preservation of the power balance, prevents the use of L-stable integrators (which limit the stiffness by introducing artificial numerical dissipation) such as the Backward Difference Formulas or Radau IIa methods [28] [29]. This imposes some restrictions on the step size or the use of adaptive strategies. However, since the average integration of the system can be interpreted as a lowpass projector and first-order anti-aliasing filter [30], parasitic oscillations at the Nyquist frequency which are typical of stiff systems are attenuated during the simulation.

Further perspectives include the use of higher-order trajectory models, exponential integrators [31] which have shown to be effective in the simulation of stiff systems and more generally Lie-group integrators [32] [33] whose trajectories belong, by construction, to the system manifold.

8. ACKNOWLEDGMENTS

The second author acknowledges the support of the ANR-DFG (French-German) project INFIDHEM ANR-16-CE92-0028.

9. REFERENCES

[1] E. S. Kuh and R. A. Rohrer, "The state-variable approach to network analysis," *Proceedings of the IEEE*, vol. 53, no. 7, pp. 672–686, 1965.

[2] C.-W. Ho, A. Ruehli, and P. Brennan, "The modified nodal approach to network analysis," *IEEE Transactions on circuits and systems*, vol. 22, no. 6, pp. 504–509, 1975.

[3] G. Hachtel, R. Brayton, and F. Gustavson, "The sparse tableau approach to network analysis and design," *IEEE Transactions on circuit theory*, vol. 18, no. 1, pp. 101–113, 1971.

[4] K. Meerkotter and R. Scholz, "Digital simulation of nonlinear circuits by wave digital filter principles," in *Circuits and Systems*. IEEE, 1989, pp. 720–723.

[5] D. T. Yeh, J. S. Abel, and J. O. Smith, "Automated physical modeling of nonlinear audio circuits for real-time audio effects–part i: Theoretical development," *IEEE transactions on audio, speech, and language processing*, vol. 18, no. 4, pp. 728–737, 2010.

[6] M. Holters and U. Zölzer, "A generalized method for the derivation of non-linear state-space models from circuit schematics," in *Signal Processing Conference (EUSIPCO), 2015 23rd European*. IEEE, 2015, pp. 1073–1077.

[7] K. J. Werner, V. Nangia, J. O. Smith III, and J. S. Abel, "Resolving wave digital filters with multiple/multiport nonlinearities," in *Proc. 18th Conf. Digital Audio Effects*, 2015, pp. 387–394.

[8] E. Hairer, C. Lubich, and G. Wanner, *Geometric Numerical Integration: Structure-Preserving Algorithms for Ordinary Differential Equations; 2nd ed.* Dordrecht: Springer, 2006.

[9] A. van der Schaft and D. Jeltsema, "Port-hamiltonian systems theory: An introductory overview," *Foundations and Trends in Systems and Control*, vol. 1, no. 2-3, pp. 173–378, 2014.

[10] A. van der Schaft, "Port-hamiltonian systems: an introductory survey," in *Proceedings of the International Congress of Mathematicians Vol. III: Invited Lectures*, Madrid, Spain, 2006, pp. 1339–1365.

[11] R. Brayton and J. Moser, "A theory of nonlinear networks. i," *Quarterly of Applied Mathematics*, vol. 22, no. 1, pp. 1–33, 1964.

[12] ——, "A theory of nonlinear networks. ii," *Quarterly of applied mathematics*, vol. 22, no. 2, pp. 81–104, 1964.

[13] A. J. van der Schaft, "On the relation between port-hamiltonian and gradient systems," *IFAC Proceedings Volumes*, vol. 44, no. 1, pp. 3321–3326, 2011.

[14] D. Jeltsema and J. M. Scherpen, "A dual relation between port-hamiltonian systems and the brayton–moser equations for nonlinear switched rlc circuits," *Automatica*, vol. 39, no. 6, pp. 969–979, 2003.

[15] A. Falaize and T. Hélie, "Simulation of an analog circuit of a wah pedal: a port-Hamiltonian approach," in *135th convention of the Audio Engineering Society*, New-York, United States, Oct. 2013, pp. –.

[16] ——, "Passive simulation of the nonlinear port-Hamiltonian modeling of a Rhodes Piano," *Journal of Sound and Vibration*, vol. 390, pp. 289–309, Mar. 2017.

[17] N. Lopes and T. Hélie, "Energy Balanced Model of a Jet Interacting With a Brass Player's Lip," *Acta Acustica united with Acustica*, vol. 102, no. 1, pp. 141–154, 2016.

[18] A. Falaize and T. Hélie, "Passive simulation of electrodynamic loudspeakers for guitar amplifiers: a port- Hamiltonian approach," in *International Symposium on Musical Acoustics*, Le Mans, France, Jul. 2014, pp. 1–5.

[19] A. Falaize and T. Hélie, "Passive guaranteed simulation of analog audio circuits: A port-hamiltonian approach," *Applied Sciences*, vol. 6, no. 10, 2016.

[20] W. Millar, "Some general theorems for non-linear systems possessing resistance," *The London, Edinburgh, and Dublin Philosophical Magazine and Journal of Science*, vol. 42, no. 333, pp. 1150–1160, 1951.

[21] C. Cherry, "Some general theorems for non-linear systems possessing reactance," *The London, Edinburgh, and Dublin Philosophical Magazine and Journal of Science*, vol. 42, no. 333, pp. 1161–1177, 1951.

[22] R. I. McLachlan, G. Quispel, and N. Robidoux, "Geometric integration using discrete gradients," *Philosophical Transactions of the Royal Society of London A: Mathematical, Physical and Engineering Sciences*, vol. 357, no. 1754, pp. 1021–1045, 1999.

[23] E. Celledoni, V. Grimm, R. McLachlan, D. McLaren, D. O'Neale, B. Owren, and G. Quispel, "Preserving energy resp. dissipation in numerical PDEs using the 'average vector field' method," *Journal of Computational Physics*, vol. 231, no. 20, pp. 6770 – 6789, 2012.

[24] B. D. Tellegen, "A general network theorem, with applications," *Philips Res Rep*, vol. 7, pp. 256–269, 1952.

[25] I. Y. Dorfman, "Dirac structures of integrable evolution equations," *Physics Letters A*, vol. 125, no. 5, pp. 240–246, 1987.

[26] T. Courant and A. Weinstein, "Beyond poisson structures," *Action hamiltoniennes de groupes. Troisieme théoreme de Lie (Lyon, 1986)*, vol. 27, pp. 39–49, 1988.

[27] P. Deuflhard, *Newton methods for nonlinear problems: affine invariance and adaptive algorithms*. Springer, 2011, vol. 35.

[28] G. Wanner and E. Hairer, *Solving ordinary differential equations II: Stiff and Differential-Algebraic Problems*. Springer, 1991, vol. 14.

[29] J. C. Butcher, *Numerical methods for ordinary differential equations*. John Wiley & Sons, 2016.

[30] R. Müller and T. Hélie, "Trajectory anti-aliasing on guaranteed-passive simulation of nonlinear physical systems," in *Proc. 20th Conf. Digital Audio Effects*, 2017.

[31] M. Hochbruck and A. Ostermann, "Exponential integrators," *Acta Numerica*, vol. 19, pp. 209–286, 2010.

[32] E. Celledoni, H. Marthinsen, and B. Owren, "An introduction to lie group integrators–basics, new developments and applications," *Journal of Computational Physics*, vol. 257, pp. 1040–1061, 2014.

[33] A. Iserles, H. Z. Munthe-Kaas, S. P. Nørsett, and A. Zanna, "Lie-group methods," *Acta numerica*, vol. 9, pp. 215–365, 2000.

A. DISCRETE GRADIENT DERIVATIVE

Proof. To prove property 4.1 for $H(x)$ a scalar potential, when the variation $\nu \neq 0$, using a) the quotient rule, b) the chain rule and c) identification with the discrete gradient definition (36), we obtain

$$\begin{aligned}\frac{\partial\overline{\nabla}H}{\partial\nu} &\overset{a}{=} \frac{[\frac{\partial}{\partial\nu}(H(x+\nu)-H(x))]\nu - [H(x+\nu)-H(x)]\frac{\partial\nu}{\partial\nu}}{\nu^2}\\ &\overset{b}{=} \frac{1}{\nu}\left(\frac{\partial H}{\partial x}(x+\nu)\frac{\partial(x+\nu)}{\partial v} - \frac{H(x+\nu)-H(x)}{\nu}\right)\\ &\overset{c}{=} \frac{\nabla H(x+\nu)-\overline{\nabla}H(x,\nu)}{\nu}.\end{aligned}$$

When $\nu \to 0$, using a) the definition of the discrete gradient (36) with b) Taylor series expansion about x and neglecting high order terms when passing to the limit leads to

$$\begin{aligned}\frac{\partial\overline{\nabla}H}{\partial\nu}(x,0) &:= \lim_{\nu\to 0}\frac{\nabla H(x+\nu)-\overline{\nabla}H(x,\nu)}{\nu}\\ &\overset{a}{=} \lim_{\nu\to 0}\frac{\nabla H(x+\nu)}{\nu} - \frac{H(x+\nu)-H(x)}{\nu^2}\\ &\overset{b}{=} \lim_{\nu\to 0}\frac{H'(x)+H''\nu}{\nu} - \frac{H'(x)\nu+H''(x)\nu^2/2!}{\nu^2}\\ &= \frac{1}{2}\frac{\partial^2 H}{\partial x^2}(x)\end{aligned}$$

□

B. DISCRETE GRADIENT OF THE DIODE POTENTIAL

Proof. Using a) the definition of the discrete gradient (36), b) the definition of the diode potential (23) followed by c) factorization of the mid-point exponential term, then d) identification of the $\sinh$ and e) sinhc functions, the discrete gradient of the diode voltage potential can be expressed as

$$\begin{aligned}\overline{\nabla}D^*(v,\delta v) &:\overset{a}{=} \frac{D_D^*(v+\delta v)-D_D^*(v)}{\delta v}\\ &\overset{b}{=} \frac{nV_T I_S}{\delta v}\left(\exp\left(\frac{v+\delta v}{nV_T}\right)-\exp\left(\frac{v}{nV_T}\right)-\frac{\delta v}{nV_T}\right)\\ &\overset{c}{=} I_S\left(\frac{nV_T}{\delta v}\exp\left(\frac{v+\delta v/2}{nV_T}\right)\left(e^{\frac{\delta v}{2nV_T}}-e^{-\frac{\delta v}{2nV_T}}\right)-1\right)\\ &\overset{d}{=} I_S\left(\frac{2nV_T}{\delta v}\exp\left(\frac{v+\delta v/2}{nV_T}\right)\sinh\left(\frac{\delta v}{2nV_T}\right)-1\right)\\ &\overset{e}{=} I_S\left(\exp\left(\frac{v+\delta v/2}{nV_T}\right)\mathrm{sinhc}\left(\frac{\delta v}{2nV_T}\right)-1\right)\end{aligned}$$

and since $\mathrm{sinhc}(0)=1$, $\overline{\nabla}D^*(v,0)=\nabla D^*(v)$ satisfies eq (33). □